PHYSICAL REVIEW B **73**, 245404 (2006)

First-principles calculations for the structural stabilities of ordered Nb_4 clusters on the Cu(111) surface

Xiaochun Wang, Qiubao Lin, Renquan Li, and Zizhong Zhu*
Department of Physics, and Institute of Theoretical Physics and Astrophysics, Xiamen University, Xiamen 361005, China

(Received 7 January 2006; revised manuscript received 13 April 2006; published 6 June 2006)

First-principles density-functional theory and supercell models are employed to study the structural stabilities and electronic structures of periodically two-dimensional arrays of Nb_4 clusters on the Cu(111) surface. The calculations on the relaxed geometries and cohesive energies show that Nb_4 clusters with both the tetrahedron and quadrangle configurations can be stably absorbed on the Cu(111) surface, which might have important applications. The absorption energies are 2.00, 1.43 eV/Nb atom for quadrangle- and tetrahedron-Nb_4 on Cu(111), respectively, showing that adsorption of quadrangle-Nb_4 clusters are more stable than those of tetrahedron-Nb_4. The energy barrier for the tetrahedron-Nb_4 adsorption to the quadrangle one is around 1.21 eV/cluster. Electronic structure calculations suggest that adsorption of Nb_4 on Cu(111) surface causes significant charge redistributions between the surface layer Cu and the Nb_4 adsorbate, leading to remarkable changes on the electronic structure of the copper surface.

DOI: 10.1103/PhysRevB.73.245404 PACS number(s): 68.43.Hn, 73.22.−f, 36.40.Qv

I. INTRODUCTION

In the last decade, fabrication and understanding of nanostructures have become an exciting area of research. This is driven by both the great potential technological applications and the scientific importance in bridging our understanding between molecules and solids. The beneficial structural, electronic, optical, magnetic, and chemical properties of nanostructures can be employed in many fields, such as in nanocatalysis,[1,2] optical and electronic devices,[3,4] single-electronic devices,[5] ultrahigh-density magnetic recording,[6–8] quantum computing and quantum cryptography.[9] Among many nanostructures on surfaces, the deposition of metal nanoclusters on oxide surfaces has been extensively investigated recently. Small metal clusters on oxide surfaces have many interesting properties and potential technological applications, such as in catalysis[10,11] and magnetic nanostructures.[12] The size and distribution of metal clusters strongly influence the functionality of the system. It has, for example, been shown that the efficiency and selectivity of metal clusters catalysts is a strong function of the size of the metal clusters, making it possible in some cases to tailor catalytic activity by varying the size of the metal clusters.[1] Although a great deal of effort has been devoted to the studies of small metal clusters on oxide surfaces,[10–15] in particular, the studies of the structural stabilities of the desired size of clusters. However, to our best knowledge, few studies have been done on the transition metal clusters on noble metal surfaces. We have, therefore, chosen to carry out our first-principles calculations on such a system. We present here the structural stabilities and electronic structures of two-dimensional arrays of small transition metal clusters Nb_4 on noble metal Cu(111) surface.

Atomic and electronic structures of transition metal clusters play an important role in understanding their growth behavior and associated catalytic, magnetic, thermal, and optical properties. Experimental studies on abundance, ionization potential (IP), photoemission, reactivity and magnetic behavior had shown size specific properties of transition metal clusters.[16] For niobium clusters, the reactivity, HOMO-LUMO gaps and the binding properties have been obtained by the experimental photoemission spectra.[17] Theoretically, the calculations have also been carried out on Nb_n with $n=2-23$ atoms.[18] The calculated second order difference in energy showed that 4-, 8-, 10-, 15-, and 16-atom clusters were magic and these should be abundant. The calculated HOMO-LUMO gap for Nb_4 was the largest among the studied clusters ($n=2-23$), indicating that Nb_4 is a highly stable cluster. The ground state of Nb_4 was shown to be a regular tetrahedron with side 2.53 Å and zero spin.[18]

The modern scanning tunneling microscopy technique allows one to manipulate the structures of small clusters on surfaces and to produce one- or two-dimensional nanostructures. On the other hand, the highly ordered two-dimensional nanostructure arrays have also been fabricated through self-organization on substrates with periodic patterns.[19] Knowledge on the cluster-substrate interactions can then help us a lot when attempting to improve the performance of the supported metal clusters as important materials. Due to the complexity of these systems, many important details of the metal clusters–metal substrate interactions are still unclear and even the cluster-substrate interfaces are only rarely known from direct measurements. On the other hand, the rapid development of computers and high-level computational methods has allowed us to perform "computer experiments" for understanding the metal cluster–metal surface interactions purely based on the computations. In this respect, *ab initio* quantum mechanical calculations can lead to important information concerning the nature and strength of the interaction, the preferred adsorption sites, the adsorption energetics, the roles of substrate and other electronic structure related properties. Since the Nb_4-Cu surface interaction involves surface chemistry (i.e., the creation or breaking of chemical bonds), a full quantum description of the system is necessary. The reasons we select Nb_4 clusters to adsorb on Cu(111) surface are due to several considerations. First, as mentioned previously, the Nb_4 is a highly stable cluster. The HOMO-LUMO gap of Nb_4 is the largest among the Nb_n ($n=2-23$). The valence electron number for Nb_4 is 20, which can fully fill a closed electron shell ($1s^2 1p^6 1d^{10} 2s^2$, according to the jellium model), showing that four is a magic number. In other words, Nb_4 cluster is a particularly strongly bound system, suggesting the importance of the atomically closed shell bcc structure.[20] Second, with four atoms, we can compare the structural stabilities of adsorbed Nb_4 with three-dimensional tetrahedron geometry and those with two-dimensional planar quadrangle geometry on the same surface. Such a comparison can provide useful information on the clusters, the surface and the interaction between them as well. Another reason for selecting a small cluster is for the saving of the computation efforts. Experimentally, the investigations for the adsorption of Nb layers on Cu(111) have been done with a specially designed UHV system equipped with a RHEED facility.[21] The Nb layers were grown by means of vacuum evaporation. The growth of Nb on the Cu(111) substrate at room substrate temperature during the deposition gave non-orientated small Nb crystal grains. Therefore, $Nb_4/Cu(111)$ could be a system with both theoretical and experimental interests. The Cu(111) surface is a well-studied surface. Atomic and electronic properties of this surface have been well documented. Copper is also an important material for structural, electrical, and electronics applications. The (111) surface of fcc copper is the most compact surface and has the lowest surface energy.[22] In the present paper, the atomic and electronic properties of the Nb_4 adsorbed on Cu(111) surface, including the preferred adsorption sites, the distortion of Nb_4 upon adsorption, the relaxation of substrate Cu(111), the adsorption cohesive energies, the charge density redistribution and the electronic density of states are calculated. Our results suggest that Nb_4 clusters are strongly bound systems and can be stably adsorbed on the Cu(111) surface, which may have important applications.

II. CALCULATIONAL METHOD

The present calculations have been performed using the Vienna *ab initio* simulation package (VASP), which is based on the density functional theory, the plane-wave basis and the projector augmented wave (PAW) representation.[23–25] The exchange-correlation effect was treated with the generalized gradient-corrected exchange-correlation functional (GGA) given by Perdew and Wang.[26,27] Periodic boundary conditions are employed and the plane wave kinetic energy cutoff employed is 26.11 Ry. In all our supercell calculations, a (3×3) surface cell of Cu(111) is used and a $3\times3\times1$ Monkhorst-Pack **k**-point mesh,[28] which corresponds to five special points in the irreducible two-dimensional Brillouin zone (BZ), are employed for the BZ integration. The total energy convergences with respect to the energy cutoff and the constant of number of k points have been tested. Optimization of the atomic structures was done by the conjugate-gradient technique, using the calculated Hellmann-Feynman forces as a guide.[29] All the atomic geometries were fully relaxed until the forces on all the atoms were less than 0.04 eV/Å.

The Cu(111) surface was modeled by repeated slabs with five copper layers separated by a vacuum region equivalent to nine copper layers. Each metal layer in the supercell contained nine Cu atoms that formed a $p(3\times3)$ surface cell. Nb_4 clusters were adsorbed symmetrically on both sides of the slab. Such a supercell can well simulate the adsorption of periodically two-dimensional arrays of Nb_4 clusters on the Cu(111) surface, including a good description of the interactions between the adsorbed clusters. All the Cu atoms were initially located at their bulk positions, with the equilibrium lattice constant of bulk determined by our calculations (the lattice constant of bulk Cu is calculated to be 3.63 Å which consists well with the value of 3.61 Å by Ref. 30). Upon Nb_4 adsorptions, all the atoms in the unit cell except for the central copper layer are fully relaxed.

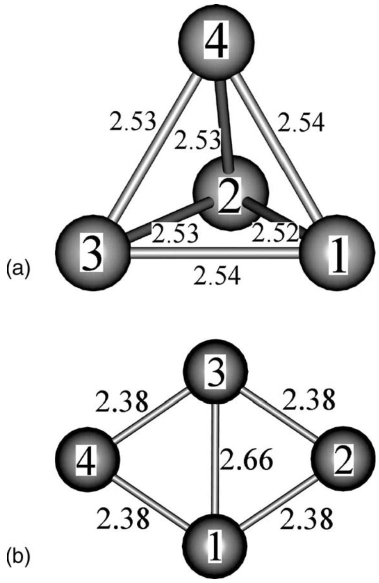

FIG. 1. (a) The lowest energy, and (b) a metastable structure of the free Nb_4 clusters. The relaxed bond lengths (Å) are also shown.

III. RESULTS AND DISCUSSIONS

We first present our calculation results for the bulk copper and the relaxed clean Cu(111) surface in order to verify our calculations. Computations for bulk Cu were performed with a cutoff energy of 26.11 Ry and a $16\times16\times16$ Monkhorst-Pack **k**-point mesh which corresponds to 408 special **k** points. We obtained a lattice constant of 3.63 Å for fcc bulk Cu, which is in good agreement with the other theoretical value of 3.61 Å (Ref. 30) and with the experimental value of 3.61 Å.[31] The clean Cu(111) surface was calculated using a 1×1 surface cell and a $8\times8\times1$ Monkhorst-Pack **k**-point mesh which corresponds to 52 special **k** points in the surface Brillouin zone. All the copper layers except for the central one were fully relaxed.

Second, we present our calculation results for the free Nb_4 clusters. The lowest energy structure (tetrahedron) and a metastable configuration (quadrangle) of the free Nb_4 clusters are plotted in Fig. 1. The corresponding structures, binding energies, HOMO-LUMO gaps and relaxed nearest neighbor bond lengths d are given in Table I. The lowest-energy Nb_4 cluster is a slightly distorted tetrahedron with sides between 2.52 to 2.54 Å. This is in good agreements with the theoretical results,[32] where sides of the distorted tetrahedron

TABLE I. The binding energies (BE, in eV/Nb atom), HOMO-LUMO gaps (eV) and the relaxed nearest neighbor bond lengths d (Å) for free Nb_4 clusters.

Nb_4		BE	Gap	d
Tetrahedron	This work	3.75	1.14	2.52–2.54
	Other theory	3.74[a]	1.20[a]	2.53,[a] 2.47,[b] 2.51–2.52[c]
	Experiments	3.90 ± 0.16[a]		
Quadrangle	This work	3.53	0.18	2.38–2.66

[a] Reference 18.
[b] Reference 33.
[c] Reference 32.

are between 2.51 Å and 2.52 Å. However, this differs from a perfect tetrahedron with side 2.47 Å obtained in Ref. 33. The calculated binding energy is 3.75 eV/atom which is also in agreement with the experimental value of 3.90 ± 0.16 eV/atom (Ref. 18) and the theoretical value of 3.74 eV/atom.[18] The calculated HOMO-LUMO gap for the tetrahedron Nb_4 cluster is 1.14 eV, as compared with the other theoretical value of 1.20 eV.[18] Results for the Nb_4 cluster in the quadrangle structure, which is less stable than the tetrahedron one, has also been listed in Table I. Results show that the binding energy of tetrahedron Nb_4 is 0.22 eV/atom larger than that of quadrangle structure (which is 3.53 eV/atom). For the quadrangle structure, the difference between the short bond length (2.38 Å) and the long bond length (2.66 Å) is much more significant than that in the tetrahedron Nb_4 cluster (2.52 Å–2.53 Å). It is known that for metals the binding energy usually increases with the increasing coordination number. We can see that the coordination of the tetrahedron structure of Nb_4 is larger than that of the quadrangle one. Both the present optimization of the atomic structure of $Nb_n(n=2-6)$ and the theoretical study for Nb_n with $n=2-23$ atoms[18] show that a free Nb_4 cluster is highly stable. The valence electron number for Nb_4 is 20, which can fully fill a closed electron shell of $1s^2 1p^6 1d^{10} 2s^2$ of the jellium model. Therefore the Nb_4 is supposed to be a magic number cluster and has high cohesive energy. Our calculations on the free Nb_4 clusters show highly directional bonding characters between Nb atoms in the Nb_4 clusters (details will be shown in the later sections) which might indicate that the jellium model could not be exactly used to explain the high-stability of Nb_4 clusters. However, jellium model had been widely used to explain the stability of metal clusters. We hope that the periodically two-dimensional arrays of Nb_4 clusters adsorbed on Cu(111) surface would be stable too.

We now turn to the properties of two-dimensional ordered Nb_4 clusters adsorbed on the Cu(111) surface. The binding energies E_b (in eV/Nb atom) and the relaxed bond lengths R (in Å) of the ordered tetrahedron- and quadrangle-Nb_4 clusters on the Cu(111) surface are shown in Table II. We have defined the binding energy for a adsorbed cluster as $E_{\mathrm{binding}}=(E_{\mathrm{total}}-E_{\mathrm{free\text{-}Nb_4}}-E_{\mathrm{clear\text{-}Cu(111)}})/2$, where E_{total} is the total energy of the adsorbed system, the $E_{\mathrm{free\text{-}Nb_4}}$ is the total energy of an independent free Nb_4 cluster, and $E_{\mathrm{clear\text{-}Cu(111)}}$ is the total energy of clean Cu(111) surface (with atomic positions relaxed). The corresponding adsorption configurations are shown in Fig. 2. The calculations on the relaxed atomic structures of Nb_4/Cu(111) show that the bottom atoms of the Nb_4 clusters prefer the hollow sites on the Cu(111) surface, for both the tetrahedron- and quadrangle-Nb_4 adsorptions. There are two types of hollow sites on Cu(111): the fcc sites and the hcp ones. The calculation on the hcp sites gives a slightly higher adsorption energy. We therefore present here only the data of the hcp sites. For tetrahedron-Nb_4/Cu(111), the Nb_4 clusters change their shapes slightly upon adsorption in order to fit the Cu(111) surface structure, for example, the equilibrium bond length R_{12} (between Nb_1 atom and Nb_2 atom, see Fig. 2) is 2.67 Å which is 0.15 Å longer than that of a free cluster (2.52 Å). Other bonds of tetrahedron-Nb_4 are also slightly changed in order to fit the substrate surface. For the quadrangle-Nb_4/Cu(111) system, the change of shape and bond lengths of Nb_4 are similar to those of tetrahedron-Nb_4/Cu(111), as described in more details in Table I and Table II. With respect to the relaxation of Cu(111) substrate upon adsorption of tetrahedron-Nb_4, the surface Cu atom which is exactly beneath the Nb_4 cluster is observed to shift its position down by 0.05 Å. On the other hand, the surface Cu atoms around the down-shifted surface Cu are observed to shift its position up by about 0.15 Å. The geometry of the surface Cu atoms beneath and around the Nb_4 cluster is like a basin.

The adsorption binding energies for the tetrahedron- and quadrangle-Nb_4/Cu(111) systems are 1.43 and 2.00 eV/Nb atom, respectively. Such a result indicates that the interactions between the quadrangle-Nb_4 clusters and the Cu(111) surface are stronger than those in the tetrahedron-Nb_4/Cu(111) system, since the binding energy for the quadrangle-Nb_4 adsorptions is larger than that of tetrahedron-Nb_4 by 0.57 eV/Nb atom. The energy barrier for the transition of the tetrahedron-Nb_4/Cu(111) system to the quadrangle-Nb_4/Cu(111) [i.e., from Fig. 2(a) to Fig. 2(c)] is

TABLE II. Binding energies E_b (eV/Nb atom) and relaxed bond lengths R(Å) of the order tetrahedron- and quadrangle-Nb_4 clusters on the Cu(111) surface.

Nb_4/Cu(111)	E_b	R_{12}	R_{13}	R_{14}	R_{23}	R_{24}	R_{34}
Tetrahedron	1.43	2.67	2.64	2.58	2.64	2.58	2.60
Quadrangle	2.00	2.49	2.76	2.48	2.52	4.14	2.49

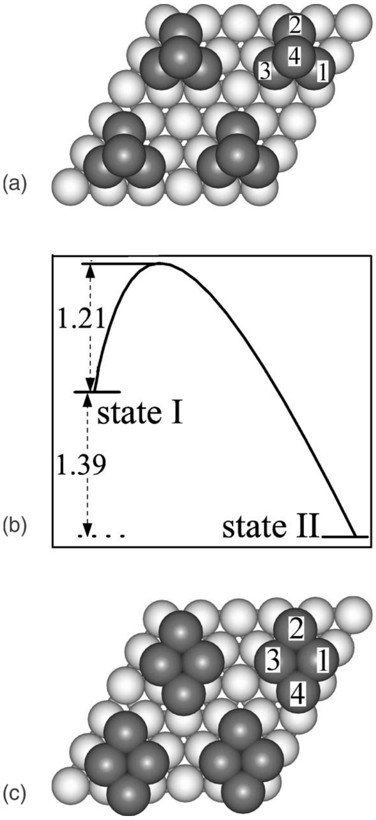

FIG. 2. (a) State-I: the periodically two-dimensional arrays of tetrahedron-Nb_4 clusters on the Cu(111) surface. (b) The potential barrier for the state-I to the state-II [i.e., the top Nb atom of the tetrahedron-Nb_4 jumping down from the (a) structure to (c)]. (c) State-II: the periodically two-dimensional arrays of quadrangle-Nb_4 clusters on the Cu(111) surface. All energies are in eV.

estimated to be 1.21 eV/cluster, which is quite noticeable. The barrier and the transition are calculated and mapped by adiabatic movement of the top Nb atom of Nb_4 from Fig. 2(a) to the plane parallel to the Cu surface, i.e., to Fig. 2(c), while keeping the positions of all the other three Nb atoms and the substrate unchanged. Although the present calculation results suggest that the quadrangle-Nb_4 clusters are now more stable than the tetrahedron-Nb_4 when absorbed on the Cu(111) surface (reminding that this is contrary to the free Nb_4, where the tetrahedron cluster is the lowest-energy structure), however, the tetrahedron-Nb_4 adsorptions should also be stable since the potential barrier between tetrahedron- and quadrangle-Nb_4/Cu(111) systems is quite noticeable. With careful deposition and under moderate temperatures, the ordered 3D tetrahedron-Nb_4 adsorptions on Cu(111) surface should be possible. Noted that for both the tetrahedron- and quadrangle-Nb_4/Cu(111) systems studied presently, the density of Nb_4 on the surface are very high which might have important applications, e.g., in the high-density memories and other developing nanostructure devices. Furthermore, although the binding energies of both the tetrahedron and quadrangle adsorptions seem to be not small, however, the values are remarkably smaller than those of free clusters. In more details, the binding energy of a free tetrahedron cluster is 3.75 eV/atom, as compared to 1.43 eV/atom for the adsorption system of tetrahedron-Nb_4/Cu(111). For the free quadrangle cluster, the binding energy is 3.53 eV/atom, compared to the 2.00 eV/atom in the quadrangle-Nb_4/Cu(111). These data imply that the interactions between atoms inside the Nb_4 clusters are significantly stronger than those between the Nb_4 clusters and the copper surface, although the Nb_4 and Cu substrate interactions seem also to be strong.

In order to see the nature of interactions between the adsorbed Nb_4 clusters and the Cu(111) surface, we plot in Figs. 3 and 4 the differences of electron charge densities for the free Nb_4 clusters and the Nb_4/Cu(111) systems. One of the contour plots of the charge density differences, which helps to visualize the characteristics of bonding, is defined as the differences between the adsorbed Nb_4/Cu(111) systems and the superposition of atomic charge densities, i.e., $\Delta\rho_1(\vec{r}) = \rho[Nb_4/Cu(111)] - \Sigma_\mu \rho_{atom}(\vec{r} - \vec{R}_\mu)$. The contour plots for the free and adsorbed tetrahedron- and quadrangle-Nb_4 clusters are presented in Fig. 3. The plane plotted is parallel to the Cu(111) surface and crossing the bottom three Nb atoms of the tetrahedron-Nb_4 or the four Nb atoms of the quadrangle Nb_4. The charge accumulation (solid lines) and depletion (dashed lines) regions relative to the noninteracting atoms are clearly shown. For the free clusters, both the tetrahedron- and quadrangle-Nb_4 show a character of strong covalent (directional) bonding between the Nb atoms inside the clusters, as seen from Figs. 3(a) and 3(c). From Figs. 3(b) and 3(d), it suggests that such a feature of strong covalent bonding has kept largely unchanged when adsorbed on the Cu(111) surface, for both the tetrahedron- and quadrangle-Nb_4. Another contour plot for the charge density differences, which will help visualize the charge transfers between the adsorbates and the substrate, is defined as the difference between adsorbed Nb_4/Cu(111) and the independent two-dimensional Nb_4 sheet and the clean Cu(111) surface, i.e., $\Delta\rho_2(\vec{r}) = \rho[Nb_4/Cu(111)] - \rho(2D - Nb_4) - \rho[Cu(111)]$. Such contours for the tetrahedron- and quadrangle-Nb_4/Cu(111) are plotted in Figs. 4(b) and 4(d). Comparatively, the Figs. 4(a) and 4(c) show their contour plots of $\Delta\rho_1(\vec{r})$. The plotted planes are now vertical to the Cu(111) surface and crossing the Nb_2 and Nb_4 atoms (see Fig. 2) of the tetrahedron-Nb_4 and the quadrangle-Nb_4. From Fig. 4, we see that directional (covalent) bonding between adsorbed Nb_4 and the Cu substrate are remarkable. Significant charge redistribution can be clearly visible between the Nb_4 adsorbate and the Cu surface layer. From Figs. 4(b) and 4(d), the plots show that the charge redistribution happened only around the surface Cu layer, i.e., electron charge densities of subsurface Cu layers are rarely disturbed upon the Nb_4 adsorption. Both the charge redistribution and charge transfer plots indicate that the interactions between the adsorbates and substrate should be strong. However, the interactions inside the Nb_4 atoms are even stronger, as already been shown by Fig. 3. The strong covalent bonding inside Nb_4 clusters accounts for the structural stability of the adsorption of Nb_4 on the Cu(111) surface, for both the quadrangle- and tetrahedron-Nb_4. The structural stability implies that Nb_4 clusters intend to remain their compactness structure on the Cu(111) and it should be possible to well identify each cluster on the surface [on the

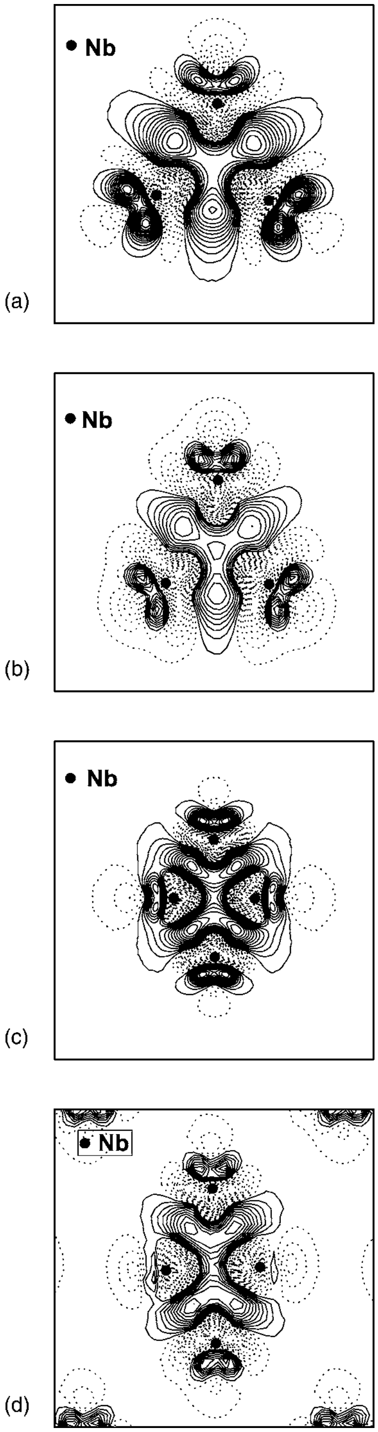

FIG. 3. Contour plots of the charge density differences (differences between an interacting system and the superposition of atomic charge densities) for (a) a free tetrahedron-Nb_4 cluster, on the plane crossing the three Nb atoms; (b) the adsorbed tetrahedron-Nb_4 cluster, on the plane parallel to the Cu(111) surface and crossing the three Nb atoms; (c) a free quadrangle-Nb_4 cluster; and (d) the adsorbed quadrangle-Nb_4 cluster. Solid and dashed lines correspond to $\Delta\rho > 0$ and $\Delta\rho < 0$, respectively.

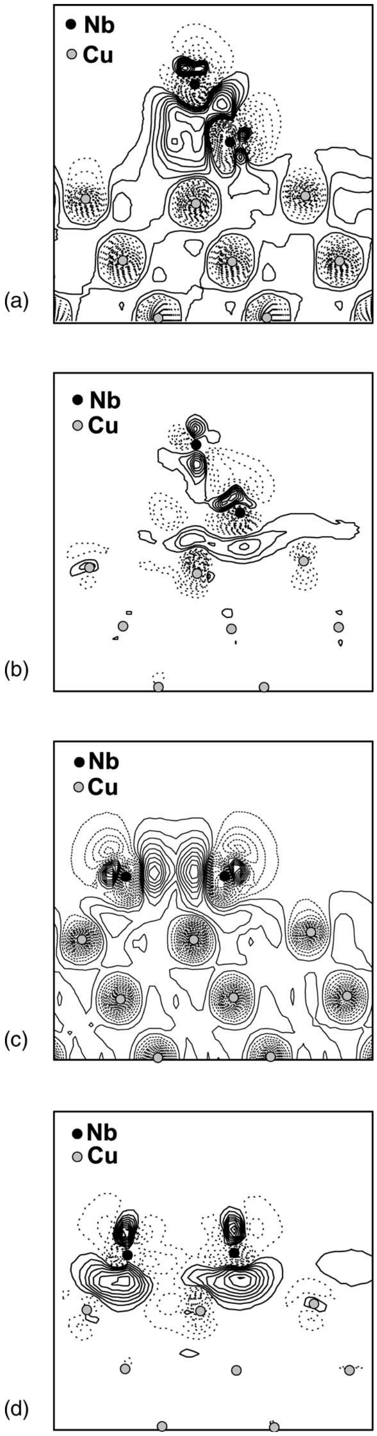

FIG. 4. Contour plots of two kinds of charge density differences (see text for detailed definitions) for (a) the $\Delta\rho_1(\vec{r})$ of the tetrahedron-Nb_4/Cu(111), the plotted plane is vertical to the Cu surface and passing Nb_2 and Nb_4 atoms; (b) the same as (a), but for $\Delta\rho_2(\vec{r})$; (c) the same as (a), but for the quadrangle-Nb_4/Cu(111); and (d) the same as (c), but for $\Delta\rho_2(\vec{r})$. Solid and dashed lines correspond to $\Delta\rho > 0$ and $\Delta\rho < 0$, respectively.

basis that Nb_4 clusters can be tightly adsorbed on Cu(111) surface]. The better stability for the adsorption of quadrangle-Nb_4 over tetrahedron-Nb_4 is simply due to the larger coordination number of Nb atoms of the quadrangle clusters when adsorbed on the Cu(111) surface, i.e., Nb in quadrangle-Nb_4/Cu(111) system has more surrounding atoms to interact with than that in the tetrahedron-Nb_4/Cu(111).

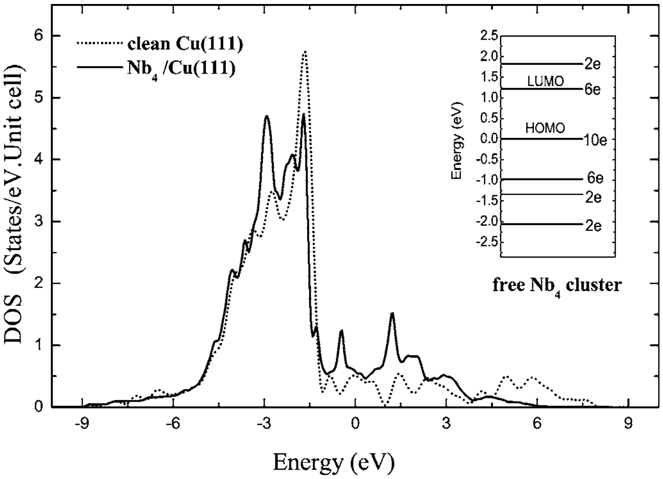

FIG. 5. Total density of states (TDOS) for the clean (dot line) and the tetrahedron-Nb_4 adsorbed Cu(111) surfaces (solid line). The electronic energy levels of the free tetrahedron-Nb_4 cluster are also plotted in the inset. The Fermi level is at 0 eV.

The calculated total electronic density of states (TDOS) for the clean and the tetrahedron-Nb_4 adsorbed Cu(111) surfaces are shown in Fig. 5. The energy levels of a free tetrahedron-Nb_4 cluster are also plotted in the inset. The variances of TDOS upon the adsorption of Nb_4 clusters are found to be mainly in the energy region higher than −4 eV (the Fermi level is set to be at 0 eV). The main feature for the TDOS after the Nb_4 adsorption is the reduction of peak at −1.7 eV and the heightening of peak at about −3.0 eV and −0.44 eV. Such a change is due to the interaction of adsorbates and the substrate, in other words, the creation of surface bonding due to adsorptions will shift some electronic states (energy levels) to the lower-energy end. In more detail, the interaction of Nb_4 clusters and the substrate shift some states at −1.7 eV to the lower-energy end of −3.0 eV. The partial density of states (PDOS) for the bottom Nb atom in the tetrahedron-Nb_4/Cu(111), for the surface Cu atom of the clean Cu(111), for the surface Cu atom of the Nb_4 adsorbed surface and for the Cu atom in the bulk are shown in Figs. 6(a)–6(c). Only the *d*-state PDOS are plotted in Fig. 6, since the values of the *s* and *p* states of the clean and adsorbed surfaces are quite small and they can be ignored relative to the *d*-PDOS. From Figs. 6(a) and 6(b), it can be seen that the main peak at −1.70 eV in Fig. 5 is mostly contributed by the *d* states of surface and bulk Cu atoms, with Nb atom's contribution negligible. The peak locating at −0.44 eV in Fig. 5, however, is mostly contributed by the *d* electrons of the Nb atom. Comparing the Figs. 6(a) and 6(b), it suggests that the adsorbate-substrate interaction can be characterized as *d*-*d* interactions, i.e., interactions mainly between the Nd *d* electrons and the Cu *d* electrons (*s* and *p* components are negligible around and below the Fermi level). It had already been shown that even for a noble metal, the *d* electrons are important for the molecule-surface interaction.[34] The comparison of *d*-band PDOS of Cu atom on the clean and adsorbed Cu(111) surfaces in Fig. 6(b) shows a remarkable change in the electronic structure of the copper surface after the Nb_4 adsorptions, suggesting strong interactions between Nb_4 and surface Cu atoms. As mentioned previously, the adsorption of Nb_4 on Cu(111) surface causes significant charge redistributions between the Nb_4 adsorbates and the surface layer Cu.

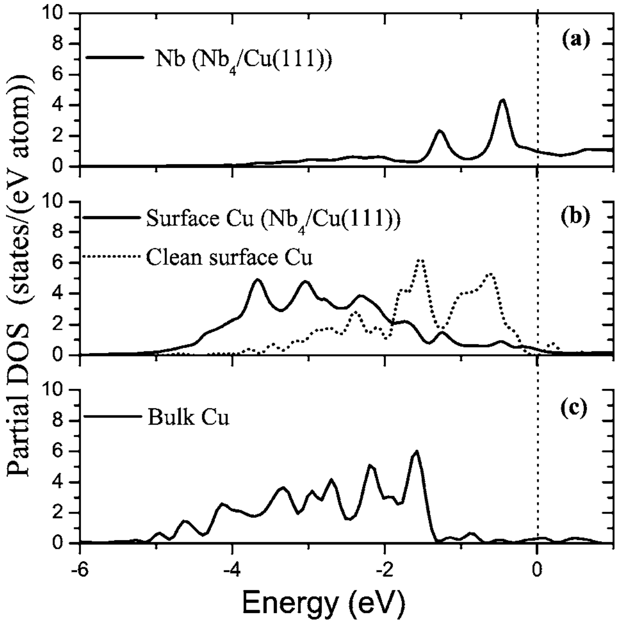

FIG. 6. The *d*-state partial DOS for (a) the bottom Nb atom of the tetrahedron-Nb_4 adsorbed on the Cu(111) surface; (b) the surface Cu atom of the clean (dot line) and the tetrahedron-Nb_4 adsorbed Cu(111) surfaces (solid line, the surface Cu atom is just beneath the atom-4 of the tetrahedron-Nb_4 cluster); (c) the Cu atom in the bulk. The Fermi level is at 0 eV.

IV. CONCLUSIONS

In summary, the supercell model combined with the first-principles density functional total energy calculations have been employed to study the structural stabilities and electronic properties of the periodically two-dimensional arrays of ordered Nb_4 clusters on the Cu(111) surface. The present calculations had shown that ordered tetrahedron- and quadrangle-Nb_4 clusters can both be stably absorbed on the Cu(111) surface, while the adsorptions with quadrangle configurations of Nb_4 are more stable. The absorption energies are 2.00 and 1.43 eV/Nb atom for the quadrangle- and tetrahedron-Nb_4 clusters on Cu(111), respectively. The energy barrier for the adsorption with tetrahedron-Nb_4 to the quadrangle ones was estimated to be 1.21 eV/cluster, which is quite noticeable. Such an energy barrier indicates that both the tetrahedron-Nb_4/Cu(111) and the quadrangle-Nb_4/Cu(111) systems should be stable and practically feasible. The high stability of the Nb_4 clusters on Cu(111) surface may have important applications, such as in the ultrahigh density memories, catalysis and nanostructure device technology.

Our results also indicate that the interactions between Nb_4 clusters and Cu(111) surface are relatively strong. The adsorption with quadrangle-Nb_4 is now more stable than that of tetrahedron-Nb_4, as compared with the free Nb_4 clusters, however, the tetrahedron-Nb_4 cluster is then more stable.

Such a change of the structure stability of Nb_4 implied a strong interaction between Nb_4 clusters and the Cu(111) surface. Even so, due to more strong covalent interactions between Nb atoms inside the Nb_4, as a consequence, the Nb_4 clusters intend to keep their compactness structure and keep a strong covalent bonding inside the Nb_4 after adsorption on the Cu(111) surface. The electronic structure calculations also show that the chemisorption of Nb_4 clusters on Cu(111) surface causes significant charge redistributions between the Nb_4 clusters and the surface layer of Cu substrate, leading to significant changes on the electronic structures of the copper surface. The interaction between the Nb_4 and the substrate is mostly contributed by the Nb-*d* and surface Cu-*d* electron interactions.

ACKNOWLEDGMENTS

This work was supported by the National Natural Science Foundation of China under Grant No. 10374076, and the Natural Science Foundation of Fujian Province under Grant No. E0320001.

---

*Corresponding author. Electronic address: zzhu@xmu.edu.cn

[1] M. Valden, X. Lai, and D. W. Goodman, Science **281**, 1647 (1998).
[2] M. Haruta, Catal. Today **36**, 153 (1997).
[3] A. O. Orlov, I. Amlani, G. H. Bernstein, C. S. Lent, and G. L. Snider, Science **277**, 928 (1997).
[4] R. P. Andres, T. Bein, M. Dorogi, S. Feng, J. I. Henderson, C. P. Kubiak, W. Mahoney, R. G. Osifchin, and R. Reifenberger, Science **272**, 1323 (1996).
[5] T. W. Kim, D. C. Choo, J. H. Shim, and S. O. Kang, Appl. Phys. Lett. **80**, 2168 (2002).
[6] S. Sun, C. B. Murray, D. Weller, L. Folks, and A. Moser, Science **287**, 1989 (2000).
[7] K. Koike, H. Matsuyama, Y. Hirayama, K. Tanahashi, T. Kanemura, O. Kitakami, and Y. Shimada, Appl. Phys. Lett. **78**, 874 (2001).
[8] T. Koide, H. Miyauchi, J. Okamoto, T. Shidara, A. Fujimori, H. Fukutani, K. Amemiya, H. Rakeshita, S. Yuasa, T. Katayama, and Y. Suzuki, Phys. Rev. Lett. **87**, 257201 (2001).
[9] P. M. Petroff, A. Lorke, and A. Imamoglu, Phys. Today **54**, 46 (2001).
[10] C. R. Henry, Surf. Sci. Rep. **31**, 231 (1998).
[11] C. T. Campbell, Surf. Sci. Rep. **27**, 1 (1997).
[12] M. Moseler, H. Hakkinen, and U. Landmann, Phys. Rev. Lett. **89**, 176103 (2002).
[13] L. J. Xu, G. Henkelman, C. T. Campbell, and H. Jonsson, Phys. Rev. Lett. **95**, 146103 (2005).
[14] S. Cai, K. M. Neyman, A. Hu, and N. Rolsch, J. Phys. Chem. B **104**, 11506 (2000).
[15] Yu. F. Zhukovskii, E. A. Kotomin, P. W. M. Jacobs, and A. M. Stoneham, Phys. Rev. Lett. **84**, 1256 (2000).
[16] V. Kumar, K. Esfarjani, and Y. Kawazoe, in *Clusters and Nanomaterials*, Springer Series in Cluster Physics (Springer-Verlag, Heidelberg, 2001), p. 9.
[17] H. Kietzmann, J. Morenzin, P. S. Bechthold, G. Gantefor, and W. Eberhardt, J. Chem. Phys. **109**, 2275 (1998).
[18] V. Kumar and Y. Kawazoe, Phys. Rev. B **65**, 125403 (2002).
[19] H. Brune, M. Giovannini, K. Bromann, and K. Kern, Nature (London) **394**, 451 (1998).
[20] R. Moro, X. Xu, S. Yin, and W. A. de Heer, Science **300**, 1265 (2003).
[21] K. Masek and V. Matolin, Vacuum **61**, 217 (2001).
[22] X. C. Wang, Y. Jia, and Q. K. Yao, Surf. Sci. **551**, 179 (2004).
[23] G. Kresse and J. Hafner, Phys. Rev. B **47**, 558 (1993).
[24] G. Kresse and J. Furthmüller, Comput. Mater. Sci. **6**, 15 (1996).
[25] G. Kresse and J. Furthmüller, Phys. Rev. B **54**, 11169 (1996).
[26] J. P. Perdew, J. A. Chevary, S. H. Vosko, K. A. Jackson, M. R. Pederson, D. J. Singh, and C. Fiolhais, Phys. Rev. B **46**, 6671 (1992).
[27] J. P. Perdew and Y. Wang, Phys. Rev. B **45**, 13244 (1992).
[28] H. J. Monkhorst and J. D. Pack, Phys. Rev. B **13**, 5188 (1976).
[29] M. C. Payne, M. P. Teter, D. C. Allan, T. A. Arias, and J. D. Joannopoulos, Rev. Mod. Phys. **64**, 1045 (1992).
[30] P. Monachesi, L. Chiodo, and R. Del Sole, Phys. Rev. B **69**, 165404 (2004).
[31] R. W. G. Wyckoff, *Crystal Structures*, 2nd ed. (Wiley, New York, 1982).
[32] H. Grõnbeck and A. Rosén, Phys. Rev. B **54**, 1549 (1996).
[33] L. Goodwin and S. R. Salahub, Phys. Rev. A **47**, R774 (1993).
[34] B. Hammer, M. Scheffler, K. W. Jacobsen, and J. K. Norskov, Phys. Rev. Lett. **73**, 1400 (1994).